1 April 2000

ELSEVIER

Optics Communications 176 (2000) 319–326

OPTICS COMMUNICATIONS

www.elsevier.com/locate/optcom

Correction of geometrical effects on fluorescence imaging of tissue

Jianan Y. Qu *, Jianwen Hua, Zhijian Huang

Department of Electrical and Electronic Engineering, Hong Kong University of Science and Technology, Clear Water Bay, Kowloon, Hong Kong, China

Received 6 October 1999; received in revised form 14 December 1999; accepted 25 January 2000

Abstract

A cross-polarization method has been used to eliminate the specular reflection and enhance the diffusive backscattering of fluorescence excitation light from tissue-like phantoms and skin tissue. We have demonstrated that the non-uniformity of excitation and collection of a fluorescence imaging system can be corrected by normalizing fluorescence signal to the cross-polarized reflection signal recorded from the same site. The ratio image of fluorescence vs. cross-polarized reflection provides a map of relative fluorescence yield over the tissue surface. This ratio imaging technique may hold the potential to detect early cancer, which usually starts from the superficial layer of tissue, based on the contrast in the fluorescence yield between early lesion and surrounding normal tissue.

PACS: 42.62.Be; 42.68.Mj; 42.30.Va
Keywords: Biological applications; Scattering; Polarization; Tissue; Spectroscopy

1. Introduction

Optical spectroscopy has been widely used in chemical analysis of biological samples. Since the mid-1980s, the use of this technology for tissue classification has become a new approach in non-invasive medical diagnostics. In particular, the methods involved with light-induced fluorescence (LIF) to characterize pathological states in human tissue have been extensively investigated. The tissues are usually classified based on the spectral characteristics of endogenous tissue fluorescence (autofluorescence). Comprehensive reviews of tissue diagnosis by the use of fluorescence spectroscopy are given in Ref. [1–3]. Careful in vivo studies on several organ sites with an optical fiber catheter revealed that the fluorescence yield of early lesions was almost always lower than that of the surrounding normal tissues, although the spectral lineshapes of early lesions and normal tissues vary both from individual to individual and within an individual [4–6]. The algorithms based on the contrast in fluorescence yield between lesion and normal tissue can be used to discriminate early lesions. However, the point by point diagnosis by the use of an optical fiber catheter of fixed fluorescence excitation and collection geometry is not easy to operate during clinical practice. An imaging technique is desirable for the clinician.

* Corresponding author. Tel.: +852-2358-8541; fax: +852-2358-1485; e-mail: eequ@ust.hk

0030-4018/00/$ - see front matter
PII: S0030-4018(00)00546-0

For examination of large areas by an imaging device, the recorded fluorescence power is strongly affected by the geometrical effects such as the separation of the source-sample–detector, incident/emission angles and irregularity of sample surface. Without a method to calibrate or compensate the geometrical effects, it is extremely difficult to compare the fluorescence yield at different sites in the imaged area, especially for in vivo measurements. Several groups have pursued different ways for mapping of fluorescence yield over the surface of turbid media. A non-imaging approach based on ratio of fluorescence intensity to reflection showed that the geometrical effects could be compensated, but the artifacts caused by the specular reflection of the tissue surface created many false positives [7,8]. In Ref. [9], an effort combining ultrasound and fluorescence spectroscopy showed that the accuracy of tissue characterization was improved by compensating for the detector–sample separation, although the dependence of fluorescence intensity on the incident/emission angle was uncertain. A digital image processing method was reported to eliminate the geometrical effects in fluorescence imaging [10]. A reference image was created by processing the raw fluorescence image with the 'moving average algorithm', a type of low pass spatial filter. A ratio image was then formed by normalizing the raw fluorescence image to the reference image. The geometrical effects in the ratio image was compensated under several restrict conditions. To ensure smoothing out the lesions and keeping the excitation and collection non-uniformities in the reference image, the algorithm requires that the lesion size is much smaller than the imaged area. Furthermore, if the spatial frequency of the geometrical artifacts overlaps with that of lesion, this low pass filter method will be invalid. In this paper we introduce a new imaging technique that allows for mapping of relative fluorescence yield over the surface of tissue by correcting the excitation and collection non-uniformities.

2. Method and materials

Our technique is based on a simple hypothesis. The light induced fluorescence and reflection of excitation light are two typical measurable of a fluorescence imaging system. The reflection of the excitation light from tissue, a kind of turbid medium, consists of three components: specular reflection, non-diffusive backscattering (such as single scattering) and diffusive backscattering. The diffusive component given by the multiple scattering of light inside tissue carries information on the illumination distribution across the tissue surface. Therefore, the geometrical effects on fluorescence measurement may be corrected by normalizing the fluorescence signal to the diffuse reflection recorded from the same site. However, the specular reflection and non-diffusive backscattering in the total reflection signal do not carry information on light propagation inside tissue. They must be removed from the reflection to ensure the validity of the geometrical correction given by normalizing the fluorescence signal to diffusive reflection. Experimentally, a cross-polarization method is proposed to reject the specular reflection and extract the diffusive components from the total reflection of excitation light. The tissue is illuminated with linearly polarized fluorescence excitation light and, by the use of a polarization analyzer, the cross-polarized image is recorded. Since forward scattering dominates the light propagation in the human tissue, the cross-polarized components in the reflection are mainly due to the multiple backscattering which produce highly diffusive reflection. The information carried in the cross polarization image are predominantly from beneath the superficial layer [11,12]. The specular reflection and superficial information (mainly due to the single backscattering), which cause the artifacts in the correction for geometrical effects, are almost completely removed in the cross-polarized image. Taking the ratio of the fluorescence signal to the cross-polarized reflection recorded from the same position, a normalized fluorescence ratio image is formed.

The experimental arrangement is shown in Fig. 1. A 100 W mercury arc lamp filtered by a band pass filter with the wavelength range from 390 to 450 nm was used as excitation source. The excitation light was delivered onto the sample through an optical fiber bundle and a linear polarizer (P1). The fluorescence and reflection signals from the sample were collected by a commercial endoscope. The angle between the optical axes of the endoscope and illumination optics was about 15°. The distance between

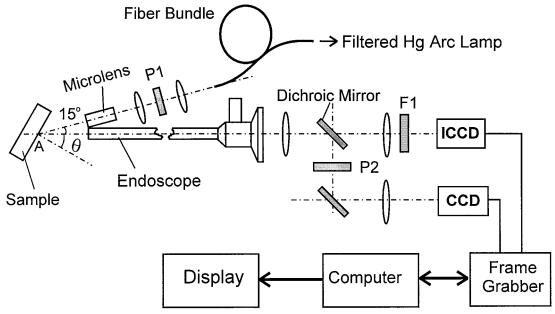

Fig. 1. Schematic diagram of the experimental setup used to collect the fluorescence and cross-polarized reflection images. θ is the angle between the optical axis of the endoscope and the normal to the sample surface.

the distal tip of endoscope and the sample was about 15 mm. The imaged area on the sample surface was about 15×15 mm at $\theta = 0°$. A dichroic mirror with cut-on wavelength at 470 nm divided the optical signal from the endoscope into the reflection and fluorescence channels. A long pass filter (F1) with cut-off wavelength at 470 nm was used to eliminate residual excitation light in the fluorescence channel. A polarizer (P2) with the polarization direction perpendicular to the polarized excitation was placed in the reflection channel to reject the specular reflection. The extinction ratio of the cross-polarized imaging channel was about 100:1. The cross-polarized reflection and fluorescence images were recorded by a CCD and intensified CCD (ICCD), respectively. The reflection and fluorescence images were digitized simultaneously by a multi-channel frame grabber at the rate of 25 frames per second. The ratio image of fluorescence against cross-polarized reflection was then generated by a PC computer.

We performed the combined cross-polarization and fluorescence imaging on tissue-simulating phantoms and living human skin. The phantoms were made of gelatin with 20% solids dissolved in boiling deionized water, polystyrene spheres (0.55 μm in diameter), fluorescent dye mixture and dominantly absorbing blood with red cells hemolyzed. The procedures to make the gel-based solid phantom are well documented [13,14]. The concentrations of blood, which determined the absorption coefficients (μ_a) of tissue phantoms used in this study, were 2.5%, 5%, and 10% volume-by-volume, respectively. The concentrations of polystyrene spheres, the dominant scatterers in the phantoms, were set to 0.25%, 0.35% and 0.5% weight-by-weight, respectively. The scattering coefficients (μ_s) and anisotropy factor (g) of tissue phantoms were calculated by Mie theory [13,15]. In the wavelength region of 450–700 nm, μ_s spectra of the tissue phantoms for three concentrations of polystyrene sphere are shown in Fig. 2 (top panel). The wavelength dependence of anisotropy factor (g) is shown in Fig. 2 (lower panel). The refractive indices of gel and polystyrene microspheres reported in Refs. [15,16] were used in the calculations. The optical properties (μ_s, μ_a and g) of all phantoms were in the range of human tissue [17]. To simulate the fluorophores in the tissue phantom, we used the mixture of green and red highly fluorescent dyes for Stabilo Boss fluorescent highlighters. The composition of fluorescent dye mixture was carefully controlled to ensure its spectral line-

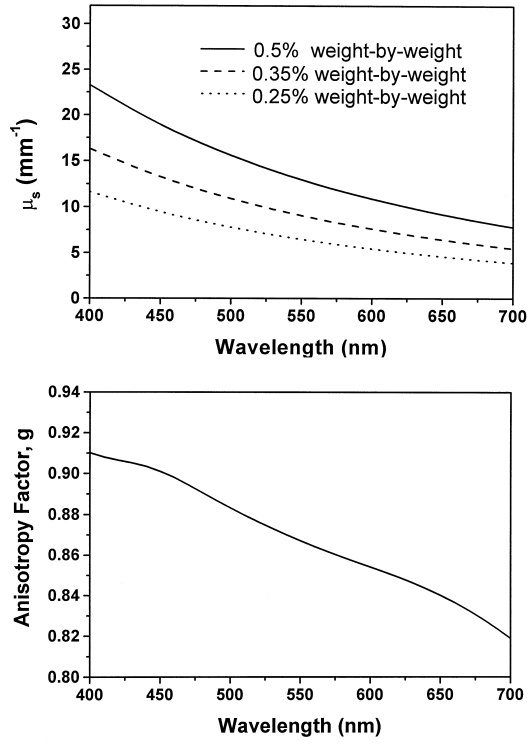

Fig. 2. (Top panel) Calculated scattering coefficients of the tissue phantoms with concentrations (w/w) of polystyrene microspheres of 0.25%, 0.35% and 5%; and (lower panel) the wavelength dependence of isotropic factor (g) of polystyrene microspheres of 0.55 μm diameter.

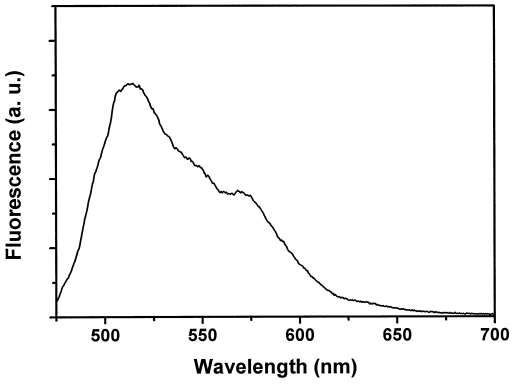

Fig. 3. Fluorescence spectrum of dye mixture.

shape to be similar to that of the autofluorescence of human tissue in the range of 450–700 nm [1–6]. The fluorescence spectrum of the dye mixture is shown in Fig. 3. It should be emphasized here that the concentration of tissue fluorescence simulating dye were kept very low since a highly sensitive ICCD was used to record the fluorescence images. The absorption of dye mixture was then much lower than that of the blood and ensured the linearity between the fluorescence yield and the dye content in the tissue phantom. For imaging of living human skin, three subjects (two Oriental and one Caucasian adults) were examined.

3. Results and discussion

In the first experiment, we demonstrate that the excitation and collection non-uniformities of fluorescence imaging can be corrected by the ratio imaging method when the optical properties of tissue phantom vary across a wide range. The compositions of the phantoms are summarized in Table 1. The concentration of fluorescence dye was kept the same. To vary the imaging geometry, the samples were rotated around the axis across the point A and perpendicular to the axes of the endoscope and illumination optics in Fig. 1. The fluorescence and cross-polarized images were collected from all tissue phantoms at $\theta = 0–60°$ with increments of 15°. The ratio image was formed by normalizing the fluorescence image to the corresponding cross-polarized reflection image and then multiplying with a fixed scaling constant. Typical raw fluorescence, cross-polarized reflection and ratio images are shown in Fig. 4 (top panel). Although the phantom was uniform, the fluorescence and cross-polarized reflection images are very inhomogeneous due to the geometrical effects. However, the ratio image appears much more uniform. This demonstrates the correction of geometrical effects on the fluorescence imaging. To evaluate the homogeneity of an image quantitatively, we normalized gray level of each pixel to the mean gray level of whole image. The histograms on fluorescence, cross-polarized reflection and ratio images with the gray level normalized are shown in Fig. 4 (lower panel). As can be seen, the gray levels of fluorescence and cross-polarized images vary widely due to the geometrical effects. In contrast, the ratio image has a

Table 1
The compositions of tissue phantoms with the same content of fluorophore

Sample number	1	2	3	4	5
Blood content (v/v %)	2.5	5	10	5	5
Microsphere content (w/w %)	0.35	0.35	0.35	0.25	0.5

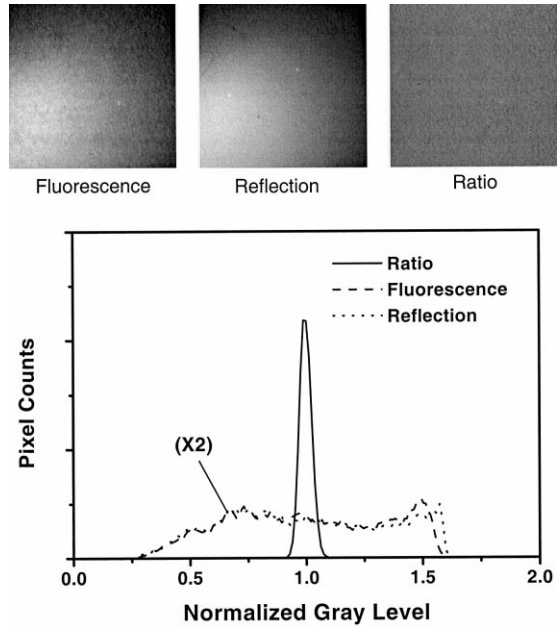

Fig. 4. Measurements on sample 2: (top panel) raw fluorescence, cross-polarized reflection and ratio images collected at $\theta = 30°$; and (lower panel) histograms on the normalized gray levels of the raw fluorescence, cross-polarized reflection ratio images.

much narrower distribution, which reflects the homogeneity of the phantom and demonstrates the correction of geometrical effects. For a quantitative comparison, we calculated the normalized standard deviations of gray level for the fluorescence, cross-polarized reflection and ratio images recorded from each phantom. The normalized standard deviation (NSD) is defined as the ratio of standard deviation over mean. The value of gray level NSD indicates the image homogeneity which is inversely proportional to the NSD value. The NSD values for the fluorescence, cross-polarized reflection and ratio images shown in Fig. 4 (top panel) are 19.5%, 20.1% and 2.8%, respectively. It was found that NSD values of fluorescence images recorded from all tissue phantoms listed in Table 1 varied from 17% to 30% at $\theta = 0–60°$, while the NSD values of all ratio images were below 4.5% and not sensitive to the angle θ except for sample 3. The NSD values for all ratio images were significantly smaller than those of raw fluorescence images. This indicates that the ratio images are much more homogeneous than raw fluorescence images, and the geometrical effects on fluorescence imaging are effectively corrected by the ratio imaging method. The relatively high NSD values for the ratio image of sample 3 was due to the poor signal to noise ratio caused by high blood content, which reduced the signal intensities of both the fluorescence and cross-polarized reflection significantly.

To demonstrate the significance to reject the artifacts caused by specular reflection, we made a comparison of the ratio images of fluorescence to reflection with and without the cross-polarization filter. The fluorescence and cross-polarized reflection image was collected by using the optical system shown in Fig. 1. The polarization filter in front of CCD was then replaced with a 0.4 OD neutral density filter for recording the total reflection image. The neutral density filter was used to compensate for the attenuation of polarization filter and keep the system responses with and without the polarizer almost identical. During the measurements, the illumination condition and the gains of the CCD and ICCD were fixed. The reflection and ratio images recorded with and without the polarization filter at $\theta = 15°$ are shown in Fig. 5. As can be seen, the specular reflection in the reflection image collected without a

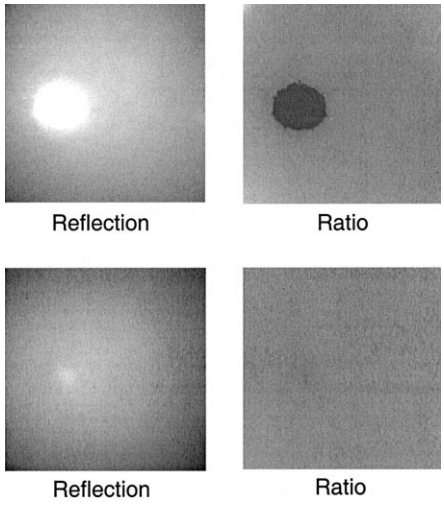

Fig. 5. Comparison of the ratio imaging with and without polarization filter: (top panels) reflection image without polarization filter and ratio image; and (lower panels) cross-polarized reflection and ratio image.

polarization filter saturates large areas of CCD. The specular reflection appears much stronger than the diffuse reflection since the endoscope of small imaging channel collects optical signal from the object in a small solid angle. In the ratio image, the specular reflection causes severe artifacts as reported in Refs. [7,8]. In contrast, the specular reflection signal was much weaker than the diffusive reflection in the cross-polarization image due to the extinction ratio of 100:1. The specular reflection artifacts have been significantly reduced. When we rotated the sample to increase the angle θ up to 45°, the specular reflection was completely moved out of the field of view. The collected total reflection without polarization filter was then given by the diffuse backscattering. We repeated the measurements with and without the polarization filter. It was found that the ratio imaging could effectively correct the geometrical effects by using either the cross-polarized reflection or total reflection. This gives more evidence that the cross-polarized reflection has the similar characteristics as the diffuse backscattering. However, it should be pointed out that the incident angle varies widely for the examination of large areas of tissue. Although total reflection can be used to correct the geometrical effects at large incident angle, the control of the illumination and collection geometry is limited in

Table 2
The gray levels of ratio images recorded from the phantoms with the compositions listed in Table 1

Sample number	1	2	3	4	5
Mean gray level	88 ± 2.6	94 ± 2.6	110 ± 8	104 ± 3.6	75 ± 2.4

clinical practice, such as endoscopy. To ensure the validity of the ratio imaging, it is essential to reject the specular reflection which is much stronger than the diffuse reflection in a small solid angle from the surface of an imaged object toward the imaging device.

The gains of the CCD and ICCD cameras were fixed for all the measurements to allow a quantitative investigation for the effect of tissue optical properties on the signal intensity of the ratio images. The mean gray levels of the ratio images recorded from all phantoms are listed in Table 2. As can be seen, the ratio was affected by the optical properties, although the content of fluorophore was fixed. The ratio increased with increasing blood content when the scattering was constant. It is known that the average absorption coefficient of blood in the excitation wavelength range (390–450 nm) is over a factor of 10 higher than in the wavelength range (470–680 nm) where the fluorescence signal was collected [18]. The excitation photon has shorter mean free path length and suffers more absorption before emerging from the tissue surface than fluorescence photon. Thus, the signal of cross-polarized reflection is more sensitive to the blood content than fluorescence. This suggests that the variation of blood content in the examined tissue area may introduce the artifact for mapping of fluorescence yield by using the ratio imaging technique. However, the sensitivity of diffuse reflection signal to the blood content in tissue could be reduced by using excitation source in the wavelength range where the blood absorption coefficients are significantly lower than that of the mercury light source used in this work. For instance, the blood absorption coefficients in the range from 460 to 480 nm are at the same level as in the wavelength range from 480 to 590 nm where most of autofluorescence are distributed [18]. Many commercial gas and solid state lasers with the emission wavelengths near 470 nm can be used as the better excitation sources than mercury lamp. The errors in fluorescence yield mapping may be reduced. Comparing the ratio images of the samples (sample 2, 4, 5) with the same blood content and different scattering property, it was found that the ratio value decreases with the increasing of scatterer concentration. This means that variation of tissue scattering property across the tissue surface may also introduce artifacts for mapping the fluorescence yield of tissue. However, the scattering coefficient is associated with the tissue structure. The artifacts caused by variation of the tissue structure across the tissue surface may provide useful information for tissue characterization.

The second experiment was designed to evaluate if the fluorescence yield can be linearly recovered by the ratio imaging technique after the correction of geometrical effects. We made four tissue phantoms with the same optical properties as sample 2 in Table 1, and the relative fluorescence dye concentrations of 0:1:2:3. The raw fluorescence, cross-polarized reflection and ratio images were generated as above. Again, the gains of CCD and ICCD were fixed to allow for the quantitative comparison of the signal intensity of ratio images. The results are shown in Fig. 6. It was found that the gelatin emitted reasonably strong fluorescence. After subtracting this background, the ratio images recorded from the phantoms with fluorescence dyes were almost linearly dependent on the dye concentration. The slight non-linearity was mainly caused by the measurement on the sample of highest dye concentration. Although the absorption of blood was dominant, the total absorption coefficient of tissue phantom was still slightly affected by

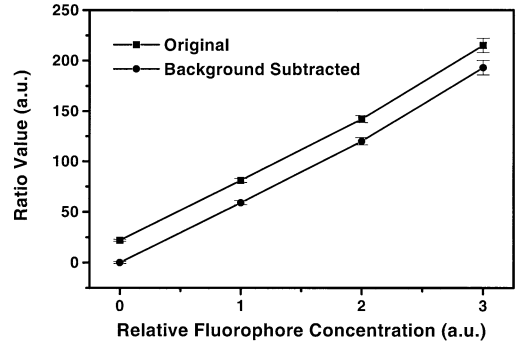

Fig. 6. Measurements of relative fluorescence yield of tissue phantoms with different concentrations of fluorophore.

the absorption of dye at high concentration level. As discussed above, the ratio value increases with the increasing of the absorption when the scattering property remains constant. The result with background subtracted in Fig. 6 indicates that the concentration of fluorescent dye in the phantom has been well recovered.

The results of the ratio imaging of simulating human tissue phantoms have shown that geometrical effects on fluorescence imaging can be corrected to a great extent. However, it should be pointed out that most of human tissues have multiply layered structure and the distribution of endogenous fluorophores is a function of depth. The phantoms used in the study were optically homogeneous. In a final experiment, we evaluated the ratio imaging method on living human skin which has very complex structure [19]. The optical properties and autofluorescence characteristics of human skin have been investigated and were found to be highly inhomogeneous [20]. The procedure to generate the ratio image of fluorescence against cross-polarization was the same as the previously. The raw fluorescence and cross-polarized reflection images were recorded on the inner forearm of three subjects. Typical results are shown in Fig. 7. The line profile analysis of the raw fluorescence, cross-polarized reflection and ratio images provides a quantitative evaluation of the correction for geometrical effects. For a fair comparison, we normalized each line profile to its mean. As can be seen, the raw fluorescence and reflection images are very inhomogeneous due to the varying separation of the source-sample–detector and incident/emission angles across the naturally curved skin surface. However, the geometrical effects are well corrected in the ratio image in spite of the fact that skin has a multiple layer structure and non-uniform distribution of fluorophores. We observed that the noise in the

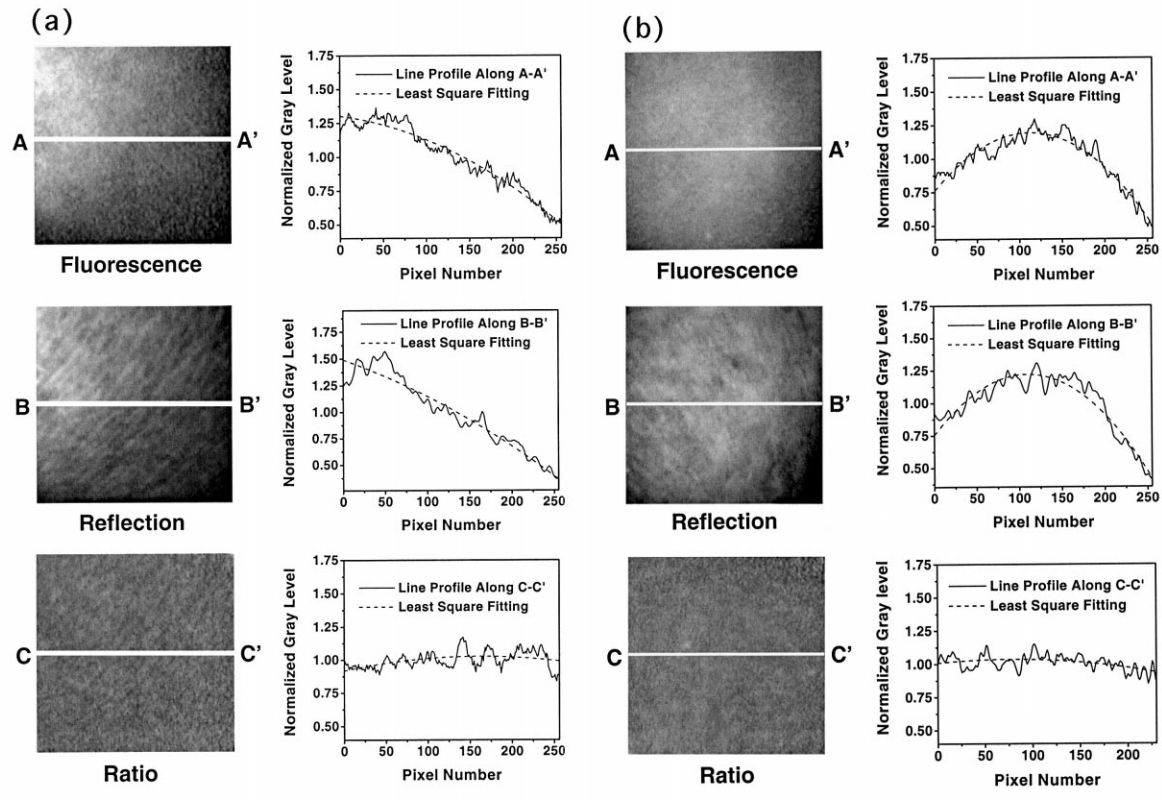

Fig. 7. Raw fluorescence, cross-polarized reflection and ratio images collected from human skin: (a) Oriental subject; and (b) Caucasian subject.

ratio image consists of both high and low frequency components. The high frequency component, caused by the electronic noise of the ICCD camera working at high gain, can be removed by using a low pass filter. The low frequency component was due to the structure of stratum and epidermis [19]. Though the cross-polarization measurement enhances the diffusive backscattering, the surface texture of the stratum and epidermal layer still appear clearly in the cross-polarized images shown in Fig. 7 because the contributions to the total reflection are from the backscattering of all skin layers. In contrast, almost no endogenous fluorescence is emitted from the stratum and epidermis, and the fluorophores are mainly distributed in the dermis which is over 100 μm beneath the skin surface [20]. Hence, the surface structures are also observable in fluorescence image, but are blurred. The difference in major signal sources between the cross-polarized reflection and fluorescence explains that the ratio image can correct the geometrical effects, but can not remove the surface structure.

In summary, we developed an imaging method to correct the geometrical effects on fluorescence imaging of tissue. The technique has been evaluated in simulating tissue phantoms with different optical properties and living human skin. The encouraging results demonstrate that the concept of ratio imaging may lead the development of a new fluorescence imaging system for detection of early lesions which have lower fluorescence yield than surrounding normal tissue. We believe that the correction of geometrical effects is due to the similar characteristics of fluorescence and cross-polarized reflection. The clear evidence has been shown in Fig. 4 (lower panel) that the histograms of fluorescence and cross-polarized reflection images are similar. The cross-polarized reflection is provided by diffusive and non-diffusive backscattering. The fluorescence emitted from the fluorescence sources in a turbid medium is diffusive. Therefore, the diffusive component in cross-polarized reflection creates the major contribution to the correction of geometrical effects. The ratio imaging technique requires that the diffusive component is much larger than the non-diffusive components in the cross-polarized reflection. This condition is generally satisfied in forward-scattering dominated turbid media (g-factor ~ 0.9 and $\mu_s \gg \mu_a$) such as human tissue. A completely quantitative explanation of our results depends on the theoretical investigation of polarized light scattering in turbid media. Extensive clinical studies are needed to evaluate the validity of this technique for imaging of diseased tissue at various organ sites.

Acknowledgements

This research is supported by Hong Kong Research Grants Council grant CA97/98.EG01 and Hong Kong University of Science and Technology.

References

[1] R. Richards-Kortum, E. Sevick-Muraca, Annu. Rev. Phys. Chem. 47 (1996) 555.
[2] S. Andersson-Engels, C. Klinteberg, K. Svanberg, S. Svanberg, Phys. Med. Biol. 42 (1997) 815.
[3] G.A. Wagnieres, W.M. Star, B.C. Wilson, Photochem. Photobiol. 68 (1998) 603.
[4] R.M. Cothren, R.R. Richards-Kortum, M.V. Sivak, M. Fitzmaurice, R.P. Rava, G.A. Boyce, G.B. Hayes, M. Doxtader, R. Blackman, T. Ivanc, M.S. Feld, R.E. Petras, Gastrointest. Endosc. 36 (1990) 105.
[5] N. Ramanujam, M.F. Mitchell, A. Mahadevan, S. Thomsen, E. Silva, R. Richards-Kortum, Gynecol. Oncol. 52 (1994) 31.
[6] J. Qu, C. MacAulay, S. Lam, B. Palcic, Opt. Eng. 34 (1995) 3334.
[7] A.E. Profio, D.R. Doiron, J. Sarnaik, Med. Phys. 11 (1984) 516.
[8] P. Lenz, Rev. Sci. Instrum. 59 (1988) 930.
[9] S. Warren, K. Pope, Y. Yazdi, A.J. Welch, S. Thomsen, A.L. Johnston, M.J. Davis, R. Richards-Kortum, IEEE Trans. Biomed. Eng. 42 (1995) 121.
[10] T.D. Wang, J. van Dam, J.M. Crawford, E.A. Preisinger, Y. Wang, M.S. Feld, Gastroenterology 111 (1996) 1182.
[11] S.G. Demos, R.R. Alfano, Appl. Opt. 36 (1997) 150.
[12] G.D. Lewis, D.L. Jordan, P.J. Roberts, Appl. Opt. 38 (1999) 3937.
[13] A.J. Durkin, S. Jaikumar, R. Richards-Kortum, Appl. Spectrosc. 47 (1993) 2114.
[14] B.W. Pogue, L. Lilge, M.S. Patterson, B.C. Wilson, T. Hasan, Appl. Opt. 36 (1997) 7257.
[15] M. Kohl, M. Essenpreis, M. Cope, Phys. Med. Biol. 40 (1995) 1267.
[16] D.W. Leonard, K.M. Meek, Biophys. J. 72 (1997) 1382.
[17] W.F. Cheong, S.A. Prahl, A.J. Welch, IEEE J. Quantum Electron. 26 (1990) 2166.
[18] O.W. van Assendelft, Spectrophotometry of Haemoglobin Derivatives, Royal Vangorcum, The Netherlands, 1970.
[19] W. Montagna, A.M. Kligman, K.S. Carlisle, Atlas of Normal Human Tissue, Springer-Verlag, New York, 1992.
[20] H. Zeng, C. MacAulay, D.I. McLean, B. Palcic, J. Photochem. Photobiol. 61 (1995) 639.